Article

Effects of Impregnation Methods and Drying Conditions on Quinoline Hydrodenitrogenation over Ni-W Based Catalysts

Fang Guo,[a,b] Shaoqing Guo,[c] Zegang Qiu,[,a] Liangfu Zhao*[a] and Hongwei Xiang[a]*

[a]*Institute of Coal Chemistry, Chinese Academy of Sciences, Taiyuan 030001, PR China*

[b]*Graduate University of the Chinese Academy of Sciences, Beijing 100039, PR China*

[c]*Taiyuan University of Science and Technology, Taiyuan 030024, PR China*

Os efeitos dos métodos de impregnação (co-impregnação e impregnação sequencial) e das condições de secagem (ar e vácuo) sobre estrutura e o comportamento catalítico de catalisadores Ni-W suportados em MCM-41 foram investigados. Os catalisadores foram caracterizados por difratometria de raios X de pó (XRD), espectroscopia de absorção no infravermelho com transformada de Fourier (FT-IR), espectroscopia de absorção no UV-Vis por refletância difusa (DRS), espectroscopia Raman, espectroscopia fotoeletrônica de raios X (XPS) e espectroscopia de absorção no infravermelho após adsorção de piridina (Py-IR). Eles foram testados para hidrodesnitrogenação (HDN) de quinolina nas temperaturas de 300-400 ºC. Os resultados de HDN mostraram que os catalisadores preparados por co-impregnação foram mais ativos do que aqueles preparados por impregnação sequencial, e que os catalisadores preparados por secagem sob vácuo foram mais ativos do que aqueles secados ao ar. A caracterização revelou que o método de co-impregnação e a secagem sob vácuo promoveram a dispersão de W, a formação de fases ativas e a formação de sítios ácidos na superfície dos catalisadores.

The effects of impregnation methods (co-impregnation and sequential impregnation) and drying conditions (air and vacuum) on the structure and catalytic behavior of MCM-41 supported Ni-W catalysts were investigated. The catalysts were characterized by powder X-ray diffraction (XRD) analysis, Fourier-transform infrared spectroscopy (FT-IR), diffuse reflectance UV-Vis absorbance spectroscopy (DRS), Raman spectroscopy, X-ray photoelectron spectroscopy (XPS) and pyridine adsorbed infrared spectroscopy (Py-IR) techniques. They were tested for hydrodenitrogenation (HDN) of quinoline at temperatures of 300-400 ºC. The HDN results showed that the catalysts prepared by co-impregnation were more active than the catalysts prepared by sequential impregnation and the catalysts prepared by drying under vacuum were more active than the catalysts dried in air. Characterization revealed that the co-impregnation method and drying under vacuum promoted the dispersion of W, the formation of the active phases, and the formation of acidic sites on the catalysts.

Keywords: Ni-W/MCM-41 catalysts, impregnation method, hydrodenitrogenation, quinoline

Introduction

The hydrotreating process is becoming an increasingly important technology for converting heavy oils to clean transportation fuels because of the shortage of light crude oils. However, most of the heavy oils have substantial amount of nitrogen compounds which are inhibitors in hydrotreating process because they can lead to the fast deactivation of hydrotreating catalysts. Meanwhile, the serious environmental pollution (NOx) can also be caused by the nitrogen compounds in oils.[1,2] Therefore, it is

necessary to remove the nitrogen compounds in heavy oils by hydrodenitrogenation (HDN) method. Thus, the development of the efficient HDN catalyst is essential.

Typical hydrotreating (including hydrodenitrogenation and hydrodesulfurization (HDS)) catalysts are alumina supported bimetallic sulfides of molybdenum or tungsten with either nickel or cobalt promoter prepared by impregnation method. In recent years, many efforts are aimed to improve the catalytic activity of the catalysts, including the use of supports such as silica-alumina, titania-alumina, zeolites and order mesoporous materials.[3-6] Among them, the support of MCM-41 which is the order mesoporous silica has attracted more and more attention due

*e-mail: qiuzegang@sxicc.ac.cn, lfzhao@sxicc.ac.cn

to the high surface areas and homogeneous pore diameters.[2] Wang *et al.* studied Ni-Mo and Ni-W sulfide catalysts supported on MCM-41 in the HDS of dibenzothiophene and the results showed that both the catalysts display high performance in HDS because the high surface area of MCM-41 favors the dispersion of active species.[7,8] Since the catalysts prepared with MCM-41 as supports exhibit good performance in HDS, they may show good properties in HDN. However, little research on their applications in HDN has been done.

Generally, the preparation method of catalysts is one of the fundamental factors that play an important role in the precursor structure of catalysts and in the activity of catalysts.[9-13] Nowadays, the impregnation method is frequently used for preparing catalysts, including co-impregnation (CI) and sequential impregnation (SI). It was reported that impregnation method significantly affected the structure, dispersion, and chemical states of Ni and Mo species on the sulfided Ni-Mo catalysts, hence affected the HDN activity for Ni-Mo based catalysts.[14,15] It was also reported that sulfided Ni-W catalysts are superior to sulfided Ni-Mo catalysts for HDN because of their high activity in hydrogenation reaction.[16] However, there has been little study about the effect of the impregnation method on the HDN activity over sulfided Ni-W based catalysts. In addition, the drying condition for the preparation of the catalyst had a significantly effect on the W species,[17] which is crucial for the hydrotreating catalyst. Based on this, the effects of the impregnation methods and drying conditions on the HDN activity over Ni-W based catalysts were investigated in the present study.

A series of MCM-41 supported Ni-W catalysts were prepared by different impregnation methods (CI and SI) and different drying conditions (air and vacuum). These catalysts were characterized by powder X-ray diffraction (XRD) analysis, Fourier-transform infrared spectroscopy (FT-IR), diffuse reflectance UV-Vis absorbance spectroscopy (DRS), Raman spectroscopy, X-ray photoelectron spectroscopy (XPS) and pyridine adsorbed infrared spectroscopy (Py-IR) techniques. The activity of HDN over the catalysts for quinoline was investigated. The relation between the structure and the catalytic activity of these catalysts in HDN of quinoline was also discussed.

Experimental

Catalyst preparation

The W precursor and Ni precursor of the catalysts were the ammonium paratungstate and nickel nitrate hexahydrate (analytical grade, produced by Sinopharm Chemical

Reagent Co., Ltd), respectively. The catalysts were prepared by co-impregnation (CI) or sequential impregnation (SI) on the MCM-41, using an equilibrium-adsorption technique. The MCM-41 was supplied by the Catalyst Plant of Nankai with a specific surface area of 1106.49 m^2 g^{-1}, a pore volume of 1.07 cm^3 g^{-1} and a Barrett-Joyner-Halenda (BJH) average pore size of 3.84 nm. For the catalysts prepared by SI, MCM-41 was first impregnated with W precursor salts solution, followed by the introduction of Ni precursor salts solution. For the catalysts prepared by CI, MCM-41 was impregnated with a solution containing a mixture of W and Ni precursors salts. After each impregnation step, the sample was aged at room temperature for 12 h, then it was dried at 80 ℃ for 12 h under air (A) or vacuum (V) condition, finally it was calcined at 540 ℃ for 3h. The amounts of WO_3 and NiO were 20 wt.% and 2.5 wt.%, respectively. The prepared catalysts were designated as Ni-W(X-Y), where X for preparation method (SI or CI) and Y means drying condition (V or A). Table 1 summarizes the preparation methods for the catalysts.

Table 1. The preparation methods for the catalysts

Catalyst	Impregnation method	Drying condition
Ni-W(CI-V)	co-impregnation	vacuum
Ni-W(CI-A)	co-impregnation	air
Ni-W(SI-V)	sequential impregnation	vacuum
Ni-W(SI-A)	sequential impregnation	air

Characterization

The physico-chemical characteristics of catalysts were characterized by XRD, FT-IR, DRS, Raman, XPS and Py-IR techniques.

XRD powder patterns were recorded on a D8 ADVANCE with Cu Kα radiation (λ = 1.54178 Å) with a scanning rate of 0.01° s^{-1}. FT-IR spectra were recorded using a Nicolet 380 spectrophotometer (4 cm^{-1} resolution and 32 scans) in dried KBr (Sigma) pellets. Diffuse reflectance UV-Vis absorbance spectra (DRS) over a range of 190-900 nm were recorded by using a Shimadzu UV-2550 spectrophotometer equipped with an integrated sphere. Laser Raman spectra were recorded on a LabRAM HR800 System with a charge-coupled device (CCD) detector at room temperature. The 325 nm of the He-Cd laser was employed as the exciting source with a power of 30 MW. Lewis and Brönsted acid sites on the surface of the catalyst were determined with FT-IR spectra of adsorbed pyridine (Py-IR). The XPS spectra were measured by using a KRATOS XSAM800 fitted with an Al Kα source (1486.6 eV) with two ultra-high-vacuum (UHV) chambers.

Catalytic activity

The quinoline HDN reaction was carried out in a fixed-bed reactor (a 50 cm long stainless steel tube with an inner diameter of 6 mm) with the feed of 0.5 wt.% N of quinoline in *n*-heptane. The reactor was charged with 1 g catalyst in 20-40 mesh size. Prior to the reaction, the catalyst was *in situ* presulfided at 400 °C and 3 MPa for 3 h with a 3 mL h^{-1} feed of 5 % CS$_2$ in *n*-hexane. After that, the HDN reaction was carried out under the conditions (pressure of 4 MPa, temperature of 300-400 °C at a step of 25 °C, weight hourly space velocity (WHSV) of 2 h^{-1} and H$_2$ feed volumetric ratio of 1000). Then after a stabilization period of 12 h, the reaction products were condensed and periodically separated from a gas-liquid separator. The reaction products were analyzed by Huaai 5860 GC gas chromatograph equipped with a flame ionization detector and a capillary column (DB-5).

Results and discussion

Dispersion of active species

The low-angle XRD patterns of the MCM-41 and the catalysts are displayed in Figure 1A. The XRD pattern of MCM-41 shows three peaks that could be indexed to (100), (110) and (200) reflections, indicating the presence of well-formed mesoporous materials with hexagonal lattice. Compared with the XRD pattern of MCM-41, the peak intensity of XRD pattern for all the catalysts diminishes. For the catalysts drying under vacuum, the (100) reflection is still observed but the intensity obviously diminished, indicating the loss of long-range order of the materials.[18,19] For the catalysts drying under air, all peaks disappear, suggesting a complete collapse of the long-range order of the materials. In conclusion, the vacuum condition is beneficial for preserving the order structure of the catalysts.

The wide-angle XRD patterns of the catalysts are presented in Figure 1B. It should be mentioned that the XRD pattern of the MCM-41 exhibits a broad signal caused by the amorphous silica walls. No crystalline phases are detected in the XRD pattern of Ni-W(CI-A) and Ni-W(CI-V), suggesting that the Ni and W species are well dispersed on the surface of the MCM-41 when the catalysts were prepared by co-impregnation method. However, the diffraction lines corresponding to the reflections of WO$_3$ (23.1, 23.6, and 24.4°) can be observed in the XRD patterns of Ni-W(SI-A) and Ni-W(SI-V), indicating that there is a poor dispersion of the WO$_3$ phase on the surface of the MCM-41 when the catalysts were prepared by sequential impregnation method. It should be noted that

the peak intensity of WO$_3$ for Ni-W(SI-V) is weaker than that for Ni-W(SI-A), which implies that the drying under vacuum favors the dispersion of W species on the surface of MCM-41. Moreover, the crystallite of Ni species cannot be detected by XRD, which indicates that the Ni species disperse much evenly with the micro-crystalline sizes less than 20 Å. This is due to that XRD is a bulk technique and is limited to crystallite sizes greater than 20 Å.[20]
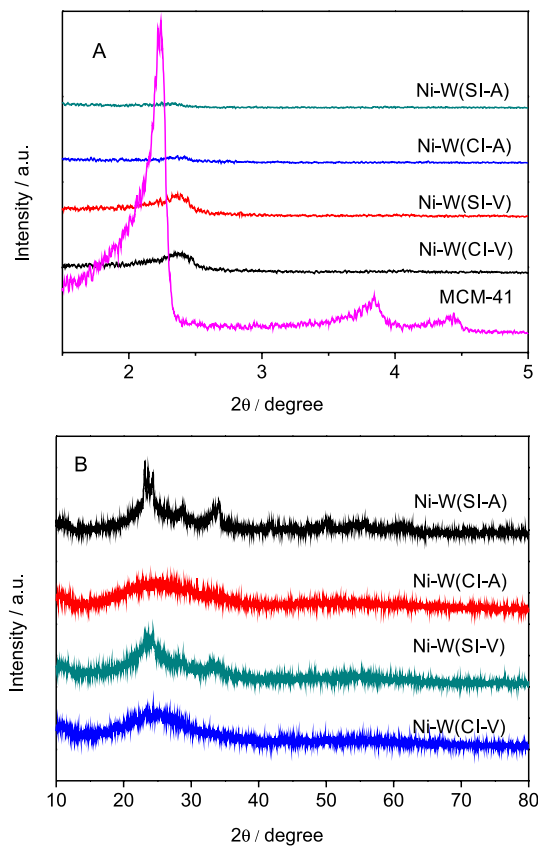

Figure 1. Low-angle and wide-angle XRD patterns of Ni-W catalysts prepared with different impregnation methods and drying conditions. (A) low-angle XRD; (B) wide-angle XRD.

Structure and chemical state of Ni and W species

The structure and chemical state of Ni and W species on catalysts were investigated by FT-IR, DRS and Raman techniques.

The FT-IR results of the MCM-41 and the catalysts are shown in Figure 2. The vibrational bands attributed to asymmetric stretching mode and symmetric stretching mode of Si–O–Si are observed in the ranges of 1300-1000 and 850-770 cm^{-1}, respectively. The vibrational bands attributed to the crystallization water molecules and the constitution water molecules are observed in the ranges of 3600-3200 and 1700-1550 cm^{-1}, respectively. In addition, the band at 974 cm^{-1} is related to the surface Si–O–H groups,

which could associate with metal compounds, inducing a high dispersion of the metal compounds on the surface of the MCM-41. The band at about 881 cm^{-1} is related to the octahedrally coordinated W species,[21] which could be easily sulfided and be involved in the genesis of active sites. From the spectra in Figure 2, it can be found that the bands of catalyst are partially or fully overlapped with those of the MCM-41. Compared with the band of Si–O–H in the MCM-41, the band of Si–O–H in the catalysts shifts to lower wavenumber and becomes broader in the catalysts because of the interaction between the silanol groups and the metal compounds.[22] It should be noted that a special band at about 881 cm^{-1} is presented in the catalysts of Ni-W(CI-A) and Ni-W(CI-V), especially for the catalyst of Ni-W(CI-V). As mentioned above, this band can be assigned to the presence of octahedrally coordinated W species and be involved in the genesis of active sites. Since the catalyst of Ni-W(CI-V) shows the greatest intensity at about 881 cm^{-1} among all the catalysts, it can be concluded that the catalyst of Ni-W(CI-V) has more active sites than the others.
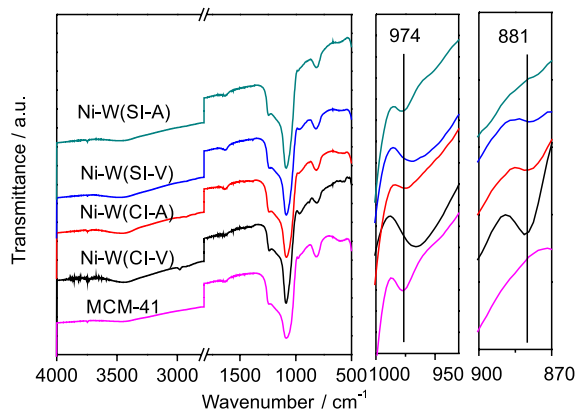

Figure 2. FT-IR spectra of the catalysts prepared with different impregnation methods and drying conditions.

The DRS spectra are illustrated in Figure 3. A broad adsorption band ranged from 200 to 350 nm is exhibited for all the catalysts, which is ascribed to tetrahedron and octahedron W species.[23] A band at about 363 nm can be assigned to the presence of bulk crystalline W oxide species.[24] A band at about 440 nm can be assigned to the d-d charge transfers in W structures associated with Ni species.[19,24] From the spectra in Figure 3, it can be found that the intensity of the band at 363 nm decreases in the order of Ni-W(SI-A) > Ni-W(SI-V) > Ni-W(CI-A) > Ni-W(CI-V). It indicates that the catalysts prepared by co-impregnation method have the well dispersed W oxide species on the surface of MCM-41, while the catalysts prepared by sequential impregnation method have the poor dispersed W oxide species on the surface of MCM-41. This

is in good agreement with the results of XRD discussed above. It is noted that a new band with maximum at about 440 nm is observed for the catalysts of Ni-W(CI-A) and Ni-W(CI-V). As mentioned above, this band is assigned to the d-d charge transfers in W structures associated with Ni species. The result indicates that the co-impregnation method favors the formation of the Ni–W–O species. Generally, the Ni–W–O species is a precursor of the active species for the catalysts in hydrotreating process. Therefore, co-impregnation method favors for the formation of active species for the catalysts.
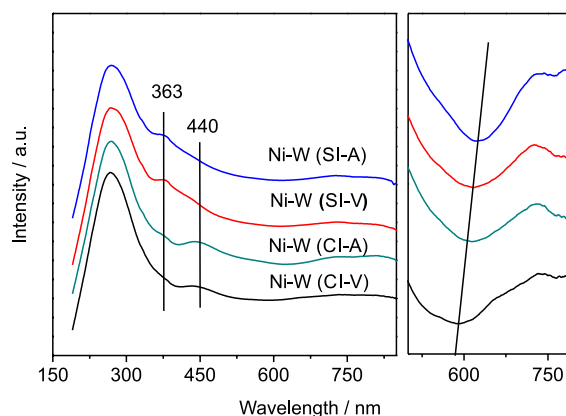

Figure 3. DRS spectra of catalysts prepared with different impregnation methods and drying conditions.

Furthermore, the broad band from 600 to 850 nm is exhibited for all the catalysts, which is associated with several Ni species and the identification of them is complicated. According to the literature,[25,26] the band in the 600-650 nm range suggests the presence of Ni^{2+} species in a tetrahedral symmetry. In this case, the Ni^{2+} species can be assigned to NiO and/or NiWO$_4$. However, the XPS results show the absence of NiO on the catalysts (see Figure 5). Therefore, the tetrahedral Ni^{2+} can be assigned to the Ni^{2+} in NiWO$_4$.

The Raman spectra are exhibited in Figure 4. It is well accepted that the standard octahedral crystalline WO$_3$ presents the bands of 804, 714 and 274 cm^{-1} while the MCM-41 does not show Raman band.[27,28] A band at 970 cm^{-1} reflects the symmetric stretching of the W=O band in octahedrally coordinated W species and a shoulder at around 811 cm^{-1} reflects the Ni–W–O stretching vibrations.[17,29] The bands of 804, 714 and 274 cm^{-1} for the crystalline WO$_3$ are not observed for catalysts of Ni-W(CI-A) and Ni-W(CI-V) in Figure 4, indicating the good dispersion of the W oxide phase on the catalysts of Ni-W(CI-A) and Ni-W(CI-V). On the contrary, the catalysts of Ni-W(SI-A) and Ni-W(SI-V) exhibit the bands of 714, 804 cm^{-1} for the crystalline WO$_3$ with strong intensity, indicating the poor dispersion of the oxide W

phase on the catalysts of Ni-W(SI-A) and Ni-W(SI-V). Meanwhile, compared with the catalyst of Ni-W(SI-V), the catalyst of Ni-W(SI-A) exhibits stronger intensity of the band at 714 and 804 cm^{-1} with a new band at 274 cm^{-1}, indicating that drying under vacuum condition benefits the dispersion of W species. It is noted that the band at 970 cm^{-1} and the shoulders at around 811 cm^{-1} are found for catalysts of Ni-W(CI-A) and Ni-W(CI-V). On the basis of the aforementioned, they can be ascribed to the octahedrally coordinated W species and Ni–W–O species on the catalysts prepared by co-impregnation, respectively. As stated in the sections of FT-IR and DRS, the octahedrally coordinated W species and the Ni–W–O species are the genesis of active species. Therefore, it can be concluded that the co-impregnation method is favorable for the formation of active species. Furthermore, the intensity of bands at 970 and 811 cm^{-1} for the Ni-W(CI-V) catalyst is stronger than that for the Ni-W(CI-A) catalyst, indicating that the drying under vacuum condition is favorable for the formation of active species on the catalysts.
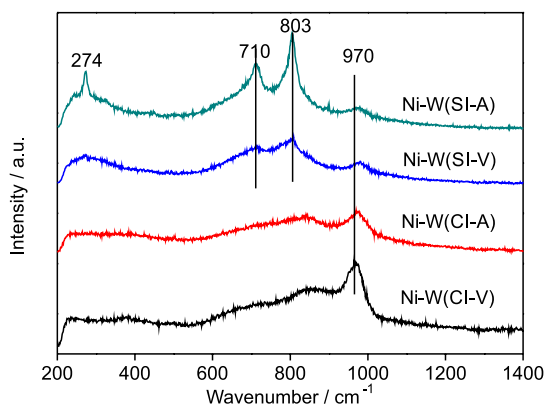

Figure 4. Raman spectra of catalysts prepared with different impregnation methods and drying conditions.

From what has been discussed above, it can be concluded that the co-impregnation method and the drying under vacuum condition favor the formation of active species on the catalysts.

Surface concentration of W species

XPS technique was performed to better understand the chemical state of Ni and W species on the catalysts and the surface concentration of W species on the catalysts. The W 4f and Ni 2p XPS spectra of all the catalysts are presented in Figure 5. The W 4f$_{7/2}$ and W 4f$_{5/2}$ doublet are presented at binding energies (BE) about 36.3 and 38.3 eV, respectively. According to the literature,[30] the BE of W 4f$_{7/2}$ spectrum in the range of 35.8-36.5 eV is ascribed to W(VI)

species. Therefore, a BE of 36.3 eV confirms the presence of W(VI) species. However, it is difficult to exactly confirm the W species by the present data because the W(VI) species includes WO$_3$ or NiWO$_4$ with similar binding energy values in this work.[31] Similarly, the Ni 2p$_{3/2}$ and Ni 2p$_{1/2}$ doublet are presented at BE about 855.7 and 873.3 eV, respectively, with the corresponding shake-up satellite at 861.9 and 880.0 eV. According to the literature,[32] the BE of Ni 2p$_{3/2}$ assigned to NiO is in the range of 853.5-854.5 eV. The lack of peak in the range of 853.5-854.5 eV for all the catalysts in this work indicates the absence of NiO on the catalysts. According to the literature,[14,33] the BE of Ni 2p$_{3/2}$ spectrum about 855.9 eV is ascribed to Ni(OH)$_2$, Ni$_2$O$_3$, and/or NiWO$_4$. However, since all catalysts were calcined at 540 °C, the presence of Ni(OH)$_2$ phase can be excluded.[15] Therefore, the Ni 2p$_{3/2}$ spectrum for the catalysts should be attributed to Ni$_2$O$_3$, and/or NiWO$_4$.
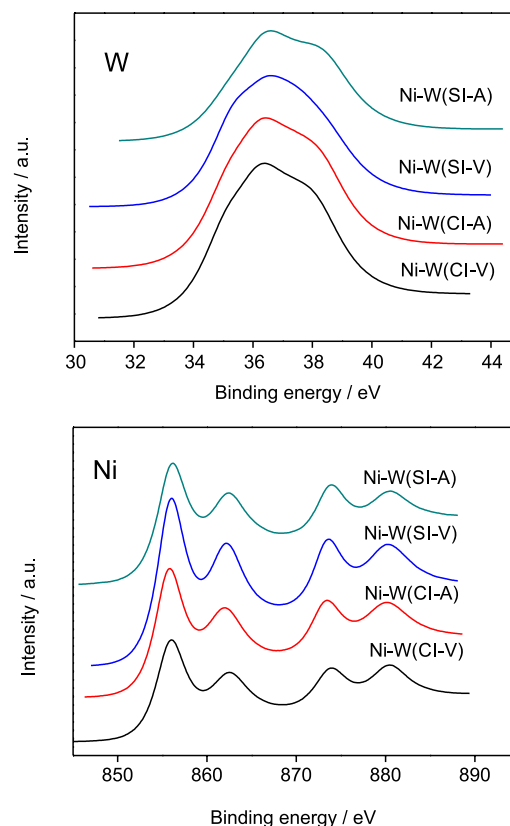

Figure 5. W 4f and Ni 2p XPS spectra of the catalysts prepared with different impregnation methods and drying conditions.

Lawrence[33] stated that the ratio of the metal-to-support from the XPS results can provide the important information about the dispersion of metal species on the surface of the support. Thus, the detailed ratio of the W/Si from the peak-fitting is listed in Table 2. Meanwhile, the BE of W 4f and Ni 2p are also listed in Table 2. It can be seen

Table 2. XPS binging energies, Cw and W/Si ratios

Catalyst	Binding energy / eV				C_W / % atoms	W/Si
	W 4f$_{7/2}$	W 4f$_{5/2}$	Ni 2p$_{3/2}$	Ni 2p$_{1/2}$		
NI-W(CI-V)	36.2	38.1	855.7	873.3	0.94	0.042
			861.9	880.0		
NI-W(CI-A)	36.3	38.3	855.9	873.8	0.84	0.038
			862.5	880.4		
NI-W(SI-V)	36.5	38.4	855.9	873.5	0.79	0.027
			862.1	880.2		
NI-W(SI-A)	36.4	38.4	856.0	873.8	0.57	0.026
			862.3	880.4		

that no significant difference can be observed in the W 4f and Ni 2p positions for all the catalysts. Furthermore, the ratio of W/Si is following the order of Ni-W(CI-V) > Ni-W(CI-A) > Ni-W(SI-V) > Ni-W(SI-A). It indicates that co-impregnation method and drying under vacuum condition favor the formation of surface W species and improve the dispersion of W species, leading to more active species on the catalysts.

Acid property of catalysts

Figure 6 shows the Py-IR spectra for the catalysts. The features of the four catalysts are very similar. The bands at 1447 and 1595 cm^{-1} (L$_1$) are ascribed to hydrogen-bonded pyridine. The bands at 1639 and 1545 cm^{-1} are ascribed to Brönsted (B) acid sites. In addition, the band at 1490 cm^{-1} indicates the formation of the adjacent Lewis and Brönsted (B+L) acid sites. Moreover, the amount of the Lewis acid sites is generally predominant. With increasing temperature, the band at 1610 cm^{-1} (L$_2$) becomes obvious, whereas the intensity of the other bands mentioned above decreased gradually, especially for L$_1$ bands. It accords with the report of Pranjal Kalita.[34] In addition, the band at 1447 cm^{-1} shifts to higher wavenumber with increasing temperature. The shift could be due to the decrease in pyridine coverage and the increase in strength of Lewis acid.[35] The amount of acid sites as a function of temperature is listed in Table 3. It clearly reveals that the acid amount follows the order of Ni-W(CI-V) > Ni-W(CI-A) > Ni-W(SI-V) > Ni-W(SI-A). Moreover, according to the acid amount at 200 or 250 °C, it can be seen that the acid strength also follows the order of Ni-W(CI-V) > Ni-W(CI-A) > Ni-W(SI-V) > Ni-W(SI-A). Because of the highest acid density and strength for Ni-W(CI-V) which is prepared by the co-impregnation method and drying under vacuum condition, it can be concluded that co-impregnation method and drying under vacuum condition can improve the acid sites on the catalyst.
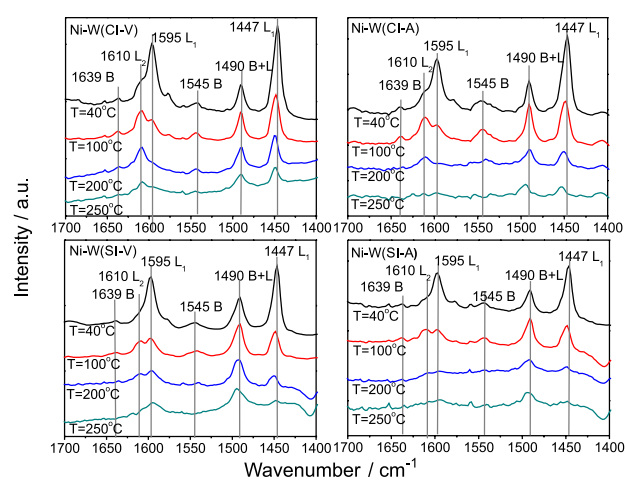

Figure 6. FT-IR spectra of pyridine adsorption combined with pyridine desorption at different temperatures on the catalysts prepared with different impregnation methods and drying conditions.
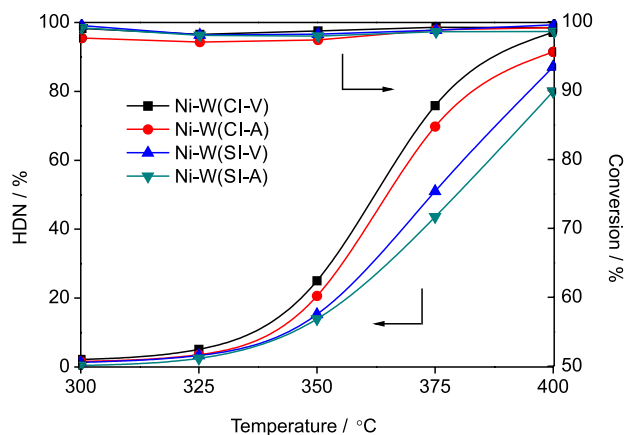
Hydrodenitrogenation activity

The effects of temperature on the conversion and the HDN of quinoline over all the catalysts are compared in Figure 7. It clearly shows that the conversion of quinoline is about 95-99% in the range of temperatures investigated but the HDN activity of quinoline is about 2-6% below the temperature of 325 °C. It indicates that quinoline could be hydrogenated easily to hydrogenation products but the reaction temperature below 325 °C may not be sufficient for the C–N band cleavage. Figure 7 also shows that the HDN activity for all the catalysts increases with increasing temperature, indicating that this reaction is activation energy demanding.[36] In addition, it can be found that the different catalysts present different HDN activity, which is in the order of Ni-W(CI-V) > Ni-W(CI-A) > Ni-W(SI-V) > Ni-W(SI-A). It is indicated that the catalysts prepared by co-impregnation method were more active than the catalysts prepared by sequential impregnation method. This agrees with the results of

Table 3. Acidity results for the Ni-W catalysts measured by FT-IR spectroscopy combined with pyridine desorption at different temperatures

Catalyst	Brönsted acidity / (µmol pyridine g⁻¹)				Lewis acidity / (µmol pyridine g⁻¹)			
	40 °C	100 °C	200 °C	250 °C	40 °C	100 °C	200 °C	250 °C
Ni-W(CI-V)	47	32	16	11	312	99	41	18
Ni-W(CI-A)	36	31	15	8	250	86	30	15
Ni-W(SI-V)	35	31	7	0	198	78	30	7
Ni-W(SI-A)	20	18	0	0	154	71	15	1

Salerno *et al.*[15] and Nava *et al.*.[11] Salerno *et al.*[15] found that the catalyst prepared by co-impregnation method of Ni and Mo was more active than those prepared by sequential impregnation method for HDS and HDN of gas oil. Nava *et al.*[11] found that the catalyst prepared by co-impregnation method of Co and Mo was more active than those prepared by sequential impregnation method for HDS of dibenzothiophene. Moreover, the HDN activity for the catalysts drying under vacuum is higher than that for the catalysts drying under air. It indicates that the catalysts drying under vacuum were more active than the catalysts drying under air. As stated previously, the catalysts prepared by co-impregnation method and drying under vacuum condition favor the fine dispersion of W species on the catalysts. The fine dispersion of W species can enhance the catalytic performance of catalysts. Moreover, the HDN activity of the catalyst is strongly dependent on the W species. As discussed above, co-impregnation and drying under vacuum condition favor the formation of octahedrally coordinated W species and Ni–W–O species, which could be more easily sulfided and are probably involved in the genesis of active sites. Furthermore, co-impregnation and drying under vacuum condition favor the formation of acid sites. In conclusion, the good HDN activity should be related with the good dispersion of W species, the appropriate nature of active species and more acid sites on the catalysts.

The HDN reaction network of quinoline is presented in Figure 8. Generally, the N in the quinoline can be removed via two pathways: the saturated intermediate pathway (Q→DHQ→PCHA→PCH+PCHE, Q: quinoline; DHQ: decahydroquinoline; PCHA: 2-propylcyclo-hexylamine; PCH: propylcyclohexane; PCHE: propylcyclohexene) and the aromatic intermediate pathway (Q→THQ1→OPA→PB, THQ1: 1,2,3,4-tetrahydroquinoline; OPA: ortho-propylaniline; PB: propylbenzene) (Figure 8).[37] In this paper, the Ni-W(CI-V) catalyst is chosen as an example to show the product distribution for HDN of quinoline because the product distribution for HDN of quinoline is similar for all the catalysts, which is shown in Figure 9. It can be seen from Figure 9 that the selectivity of THQ1 is much

Figure 7. Effect of temperature on the conversion and HDN of quinoline: influence of the impregnation method and drying condition. Reaction conditions: p = 4 MPa, H₂ feed ratio = 1000, WHSV = 2 h⁻¹.

higher than that of 5,6,7,8-tetrahydroquinoline (THQ5) at lower temperature. It indicates that the hydrogenation of quinoline to THQ1 is much easier than the hydrogenation of quinoline to THQ5, since the heterocyclic ring is more easily hydrogenated than the benzenoid ring. With increasing temperature, the selectivity of THQ1 decreases dramatically while the selectivity of DHQ and THQ5 goes through a maximum at 350 °C then decreases. In fact, the C–N band cleavage is the rate-determining step at lower temperatures. Therefore, the further reaction of DHQ and THQ5 is limited at lower temperatures. Meanwhile, the formation of DHQ and THQ5 increases with the increasing temperature below 350 °C. Consequently, the selectivity of DHQ and THQ5 is increased with the increasing temperature below 350 °C. However, the C-N band cleavage is significantly accelerated with further increasing temperature.[38] But the hydrogenation reaction is inhibited at high temperature because it is an exothermic reaction. So the selectivity of DHQ and THQ5 decreases with further increasing temperature. The selectivity of OPA and PCHA is negligible, revealing that the further reaction rate of OPA and PCHA is faster than the cracking rate of THQ1. The selectivity for the final products of PCH, PCHE and PB continuously increases with increasing temperature. The increase of PCH and PCHE is more significant than that of PB from
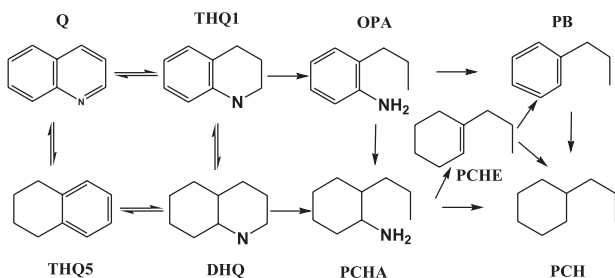
Figure 8. HDN reaction network of quinoline. Q, quinoline; THQ5, 5,6,7,8-tetrahydroquinoline; DHQ, decahydroquinoline; THQ1, 1,2,3,4-tetrahydroquinoline; OPA, ortho-propylaniline; PCHA, 2-propylcyclo-hexylamine; PCHE, propylcyclohexene; PCH, propylcyclohexane; PB, propylbenzene.
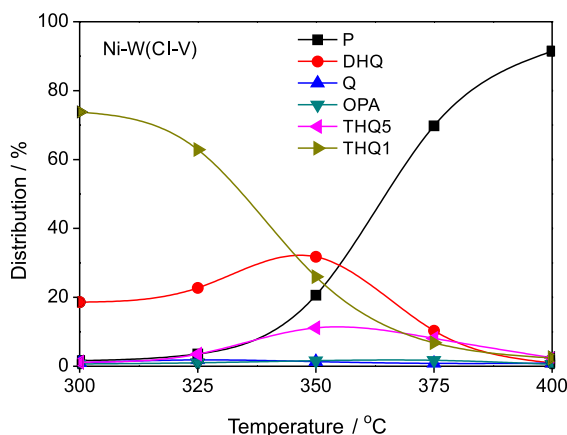

Figure 9. Product distribution for HDN of quinoline on Ni-W(CI-V) at different reaction temperatures. Reaction is conducted at p = 4 MPa, H_2 feed ratio = 1000, WHSV = 2 h^{-1}.
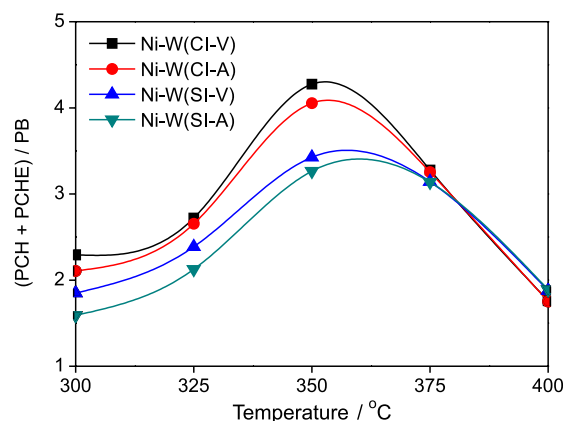

Figure 10. (PCH+PCHE)/PB ratio of catalysts prepared with different impregnation methods and drying condition at different reaction temperatures. Reaction is conducted at p = 4 MPa, H_2 feed ratio = 1000, WHSV = 2 h^{-1}.

300 to 350 °C. However, PCH and PCHE increase less significantly than PB from 350 to 400 °C. These lead to the observation that the (PCH+PCHE)/PB ratio (Figure 10) goes through a maximum at 350 °C, which is in agreement with Lee *et al.*.[39]

Conclusions

A series of Ni-W based catalysts were prepared by two impregnation methods (co-impregnation and sequential impregnation) and two drying conditions (air and vacuum). The HDN activity was investigated over the Ni-W based catalysts. The results showed that the Ni-W(CI-V) catalyst prepared by co-impregnation and drying under vacuum exhibited the best HDN activity among all the catalysts investigated. Its superior HDN activity was due to the good dispersion of the W species, the appropriate nature of the active species and the higher number of acid sites on the catalyst.

Acknowledgements

References

1. Choudhary, T. V.; Parrott, S.; Johnson, B; *Catal. Commun.* **2008,** *9*, 1853.

2. Lei, Z. P.; Gao, L. J.; Shui, H. F.; Chen, W. L.; Wang, Z. C.; Ren, S. B.; *Fuel Process. Technol.* **2011**, *92*, 2055.

3. Fernandez-Vargas, C.; Ramirez, J.; Gutierrez-Alejandre, A.; Sanchez-Minero, F.; Cuevas-Garcia, R.; Torres-Mancera, P.; *Catal. Today* **2008**, *130*, 337.

4. Grzechowiak, J. R.; Wereszczako-Zielińska, I.; Mrozińska, K.; *Catal. Today* **2007**, *119*, 23.

5. Ding, L. H.; Zheng, Y.; Yang, H.; Parviz, R.; *Appl. Catal. A.* **2009**, *353*, 17.

6. Pawelec, B.; *J. Catal.* **2004**, *223*, 86.

7. Wang, A. J.; Wang, Y.; Toshiaki, K.; Chen, Y. Y.; Atsushi, I.; *J. Catal.* **2002**, *210*, 319.

8. Wang, A. J.; Li, X.; Chen, Y. Y.; Han, D. F.; Wang, Y.; Hu, Y. K.; Toshiaki, K.; *J. Catal.* **2001**, *199*, 19.

9. Maity, S.; Flores, G.; Ancheyta, J.; Rana, M.; *Catal. Today* **2008**, *130*, 374.

10. Pawelec, B.; Halachev, T.; Olivas, A.; Zepeda, T. A.; *Appl. Catal., A* **2008**, *348*, 30.

11. Nava, R.; Morales, J.; Alonso, G.; Ornelas, C.; Pawelec, B.; Fierro, J. L. G. A.; *Appl. Catal., A* **2007**, *321*, 58.

12. Papadopoulou, C.; Vakros, J.; Matralis, H. K.; Kordulis, C.; Lycourghiotis, A.; *J. Colloid Interface Sci.* **2003**, *261*, 146.

13. Okamato, Y.; Ishihara, S. Y.; Kawano, M.; Satoh, M.; Kubota, T.; *J. Catal.* **2003**, *217*, 12.

14. Sardhar Basha, S. J.; Vijayan, P.; Suresh, C.; Santhanaraj, D.; Shanthi, K.; *Ind. Eng. Chem. Res.* **2009**, *48*, 2774.

15. Salerno, P. A.; *Appl. Catal., A* **2004**, *259*, 17.

16. Luan, Y. Z.; Zhang, Q. M.; He, D. M.; Guan, J.; Liang, C. H.; *Asia-Pac. J. Chem. Eng.* **2009**, *4*, 704.

17. Benitez, V. M.; Figoli, N. S.; *Catal. Commun.* **2002**, *3*, 487.

18. Carriazo, D.; Domingo, C.; Martín, C.; Rives, V.; *J. Solid State Chem.* **2008**, *181*, 2046.

19. Palcheva, R.; Spojakina, A.; Dimitrov, L.; Jiratova, K.; *Microporous Mesoporous Mater.* **2009**, *122*, 128.

20. Li, C. P.; Proctor, A.; Hercules, D. M.; *Appl. Spectrosc.* **1984,** *38,* 880.

21. Khder, A. E. R. S.; Hassan, H. M. A.; El-Shall, M. S.; *Appl. Catal., A* **2012**, *411-412*, 77.

22. Park, S. J.; Lee, S. Y.; *J. Colloid Interface Sci.* **2010**, *346*, 194.

23. Benitez, A.; Ramirez, J.; Fierro, J. L. G.; Lopez Agudo, A.; *Appl. Catal., A* **1996**, *144*, 343.

24. Duan, A. J.; Gao, Z. Y.; Huo, Q.; Wang, C. Y.; Zhang, D. Q.; Jin, M. C.; Jiang, G. Y.; Zhao, Z.; Pan, H. F.; Chung, K.; *Energy Fuels* **2010**, *24*, 796.

25. Li, X.; Zhou, F.; Wang, A. J.; Wang, L. Y.; Hu, Y. K.; *Ind. Eng. Chem. Res.* **2009**, *48*, 2870.

26. Li, D.; Nishijima, A.; Morris, D. E.; *J. Catal.* **1999,** *182*, 339.

27. Chen, H.; Dai, W. L.; Deng, J. F.; Fan, K. N.; *Catal. Lett.* **2002**, *81,* 131.

28. Zhang, Z. R.; Suo, J. S.; Zhang, X. M.; Li, S. B.; *Appl. Catal., A* **1999**, *179*, 11.

29. Soni, K.; Boahene, P. E.; Chandra Mouli, K.; Dalai, A. K.; Adjaye, J.; *Appl. Catal., A* **2011**, *398*, 27.

30. Le, Z.; Afanasiev, P.; Li, D. D.; Long, X. Y.; Vrinat, M.; *Catal. Today* **2008**, *130*, 24.

31. Ding, L. H.; Zheng, Y.; Zhang, Z. S.; Ring, Z.; Chen, J. W.; *Catal. Today* **2007**, *125*, 229.

32. Liu, F.; Xu, S. P.; Cao, L.; Chi, Y.; Zhang, T.; Xu, D. F.; *J. Phys. Chem. C* **2007**, *111*, 7396.

33. Lawrence, S. J.; Makovsky Leo, E.; Stencel, J. M.; Brown, F. R.; David, M. H.; *J. Phys. Chem.* **1981**, *85*, 3700.

34. Kalita, P.; Gupta, N.; Kumar, R.; *J. Catal.* **2007**, *245*, 338.

35. Ferdous, D.; Bakhshi, N. N.; Dalai, A. K.; Adjaye, J. A.; *Appl. Catal., B* **2007**, *72,* 118.

36. Suresh, C.; Santhanaraj, D.; Gurulakshmi, M.; Deepa, G.; Selvaraj, M.; Sasi Rekha, N. R.; Shanthi, K.; *ACS Catal.* **2012**, *2,* 127.

37. Li, Y. P.; Liu, D. P.; Liu, C. G.; *Energy Fuels* **2010**, *24*, 789.

38. Fan, X.; Liu, G. F.; Zong, Z. M.; Zhao, X. Y.; Cao, J. P.; Li, B. M.; Zhao, W.; Wei, X. Y.; *Fuel Process. Technol.* **2013**, *106*, 661.

39. Lee, R. Z.; Zhang, M. S.; Ng, F. T. T.; *Top. Catal.* **2006**, *37,* 121.